Available online at www.sciencedirect.com

SCIENCE DIRECT

Microchemical Journal 81 (2005) 122–132

MICROCHEMICAL JOURNAL

www.elsevier.com/locate/microc

Special article

Determination of adsorption and speciation of chromium species by saltbush (*Atriplex canescens*) biomass using a combination of XAS and ICP–OES

M.F. Sawalha[a], J.L. Gardea-Torresdey[a,b], J.G. Parsons[b], Geoffrey Saupe[b], J.R. Peralta-Videa[b,*]

[a]*Environmental Science and Engineering PhD Program, The University of Texas at El Paso, 500 West University Avenue, El Paso, TX 79968-0513, USA*
[b]*Department of Chemistry, The University of Texas at El Paso, 500 West University Avenue, El Paso, TX 79968-0513, USA*

Received 21 January 2005; accepted 22 January 2005
Available online 19 March 2005

Abstract

Studies were performed to determine the effect of pH on chromium (Cr) binding by native, esterified, and hydrolyzed saltbush (*Atriplex canescens*) biomass. In addition, X-ray absorption spectroscopy studies were performed to determine the oxidation state of Cr atoms bound to the biomass. The amounts of Cr adsorbed by saltbush biomass were determined by inductively coupled plasma–optical emission spectroscopy (ICP–OES). For Cr(III), the results showed that the percentages bound by native stems, leaves, and flowers at pH 4.0 were 98%, 97%, and 91%, respectively. On the other hand, the Cr(VI) binding by the three tissues of the native and hydrolyzed saltbush biomass decreased as pH increased. At pH 2.0 the stems, leaves, and flowers of native biomass bound 31%, 49%, and 46%, of Cr(VI), respectively. The results of the XAS experiments showed that Cr(VI) was reduced in some extend to Cr(III) by saltbush biomass at both pH 2.0 and pH 5.0. The XANES analysis of the Cr(III) reaction with the saltbush biomass parts showed an octahedral arrangement of oxygen atoms around the central Cr(III) atom. The EXAFS studies of saltbush plant samples confirmed these results.

Keywords: Saltbush; Chromium binding; EXAFS; XANES; ICP–OES

1. Introduction

Heavy metals tend to accumulate in the environment causing various diseases and disorders in living organisms [1]. Cr enters into water resources from industrial processes such as electroplating, tanning, dyeing, and printing [2]. This metal usually occurs in trivalent or hexavalent oxidation states in soil and water [3,4]. Although both Cr species are toxic, hexavalent Cr poses a greater health risk than trivalent due to its carcinogenic activity [5,6]. Because of this, many researchers have focused on Cr removal from soil and water [4,7–9]. The conventional metal removal procedures include filtration, flocculation, reverse osmosis, solvent extraction, and ion exchange resins. In general, these techniques are associated with high energy requirements, incomplete removal, generation of wastes that requires special disposal, and potential health risks [10,11]. The most common treatment for Cr in industrial effluents involves the reduction of Cr(VI) to the less toxic Cr(III), the recipitation of Cr(III) into $Cr(OH)_3$ at high pH values, and the separation of the precipitate. This procedure has been found to be expensive and produces contaminated wastes [4,7].

The use of dead plant biomass (some times referred to as phytofiltration) has appeared as an option for metal removal from contaminated waters. This material has a low cost, is abundant, and it could be selective for an easy metal removal [1,10–14]. Previous studies on Cr removal indicate that certain biomasses such as alfalfa, hops, algae and others, have a high capacity for chromium binding. Experimental results demonstrated that Cr(III) and Cr(VI) bind to the stems and leaves of hops biomass through oxygen atoms [15]. Another study suggested that, while the

* Corresponding author. Tel.: +1 915 747 8998; fax: +1 915 747 5748.
E-mail address: jperalta@utep.edu (J.R. Peralta-Videa).

0026-265X/$ - see front matter © 2005 Elsevier B.V. All rights reserved.
doi:10.1016/j.microc.2005.01.008

binding for Cr(III) by oat biomass (*Avena monida*) occurs through negatively charged ligands such as carboxylic groups, the binding of Cr(VI) may occurs via positively charged ligands such as amino groups [16]. It has also been proposed that Cr binding to the biomass might be due to ligand exchange, ion exchange, and reduction mechanisms [17]. Nevertheless, the mechanism involved in Cr binding by biomass is not fully understood.

The use of saltbush plant (*A. canescens*) for phytofiltration has not been previously studied. This plant could be promising, since *Atriplex* species have special bladders in the leaves that act as salt sinks for the removal of the excess of salt [18]. In the present research study, we investigated the potential use of saltbush biomass for the removal of Cr(III) and Cr(VI) from aqueous solutions. Chemical modification was used to investigate the potential involvement of carboxyl groups on saltbush biomass in Cr(III) and Cr(VI) binding [14–16].

Extended X-ray absorption fine structure (EXAFS) was used to provide information about the coordination environment and the nearest neighboring atoms and the ligands involved in the binding of Cr by saltbush biomass. In addition, X-ray absorption near edge structure (XANES) was used to provide information about possible changes in the oxidation of Cr atoms bound to the biomass. The results of these studies are reported herein.

2. Experimental

2.1. Collection and preparation of saltbush biomass

Saltbush plants were collected from wild areas around El Paso, Texas USA. The plants were washed with tap water and separated into flowers, stems, and leaves. All samples were oven dried at 90 °C for 1 week, and the different portions of the plant were then ground using a Wiley mill, to pass through a 0.149-mm (100-mesh) sieve.

2.2. Esterification of saltbush biomass

Carboxyl groups of the biomass were esterified following a similar method previously described [19,20]. Nine grams of saltbush biomass were washed with 0.01 M HCl and with deionized water (DI) to remove any debris and soluble impurities. The biomass was suspended in 633 ml of 99.9% methanol (HPLC grade) and 5.4 ml of concentrated HCl was added to give a final acidic concentration of 0.1 M HCl. While continuously stirring, the solution was heated to 60 °C for 48 h. The biomass was then pelleted by centrifugation at 3000 rev. min^{-1} for 5 min using a Fisher Scientific Marathon 6 K centrifuge, and the supernatant was decanted, dried, and weighed to account for possible loss of biomass. The biomass was then washed three times with DI water to quench the reaction. Subsequently, the biomass was lyophilized and used in batch Cr binding experiments.

2.3. Hydrolysis of saltbush biomass

Base hydrolysis of saltbush biomass was performed as previously described in the literature [21,22]. After washing the biomass, as previously mentioned, the 9 g of biomass was reacted with 100 ml of 0.1 M sodium hydroxide for a period of 1 h at room temperature. The hydrolysis reaction was quenched by washing the biomass with DI water three times, and then the biomass was lyophilized for further batch experiments.

2.4. pH Profile batch experiments

These experiments were performed following the method previously published [12]. A 250-mg mass of saltbush biomass (either native, esterified or hydrolyzed) was washed twice with 0.01 M HCl. The washings were decanted, dried, and weighed to account for any loss of biomass. Each biomass sample was resuspended in 50 ml of DI water making biomass slurry of approximately 5-mg biomass per ml of water. Separate solutions of 0.1 mM Cr(III) or Cr(VI) were prepared from the corresponding salts: $Cr(NO_3)$ and $K_2Cr_2O_7$. The biomass slurry was adjusted to the following pH values: 2.0, 3.0, 4.0, 5.0, and 6.0. At each pH, a 2-ml aliquot was extracted in triplicate, transferred to clean 5-ml tubes, and centrifuged at 3000 rpm for 5 min. The supernatants were discarded and the biomass was saved for further use. After centrifugation, 2.0 mL of the respective pH adjusted Cr solution (either Cr(III) or Cr(VI)) was added to the respective pH adjusted biomass samples. In addition, at each pH of reaction, control samples consisting of the metal solution were created. Both the biomass and control samples were equilibrated on a rocker for 1 h and subsequently centrifuged at 3000 rpm for 5 min; the supernatants were kept for metal determination. The difference in chromium concentration between the controls and the reacted samples was assumed to be the amount of metal bound to the biomass.

2.5. Chromium binding capacity studies

The method used to determine the binding capacity of chromium to saltbush biomass was performed as reported previously in the literature [21]. In this study, after washing each type of biomass with HCl and DI water as previously mentioned, the biomass samples in triplicate (5 mg ml^{-1}, pH 5.0) were resuspended in a 3.0 mM solution of either Cr(III) or Cr(VI) buffered at pH 5.0. The suspensions were shaken for 10 min, centrifuged, and decanted. The supernatants were kept for Cr analysis. The same biomaterials were resuspended several times with a fresh aliquot of the 3.0 mM Cr solution. The procedures of reacting, centrifuging, and suspending were repeated until the biomass was saturated (i.e. the metal concentration in the supernatant was the same as the initial solution). In addition, control samples were also created using only the 0.3 mM chromium solution. The controls and

reaction samples were treated alike. The samples were diluted as required and analyzed for Cr content. The capacity was assumed to be the difference between the control samples and the reaction samples of each reaction cycle and was calculated using a sum of the individual cycles.

2.6. Metal quantification

A Perkin Elmer 4300 DV inductively coupled plasma/optical emission spectrometer (ICP–OES) (Perken Elmer Corporation, Shelton, CT) was used to analyze the samples resulted from the pH and capacity studies. Table 1 shows the operational parameters for the ICP–OES used in the analysis of the Cr binding to saltbush biomass. The instrument was calibrated from 1.0 mg ml^{-1} to 6.0 mg ml^{-1} for the pH studies and from 1.0 mg ml^{-1} to 20.0 mg ml^{-1} for the capacity studies. Calibration coefficients obtained for all analysis were 0.999 or better.

2.7. XAS experiments

2.7.1. XAS sample preparation

A solution of 1000–mg ml^{-1} Cr(III) or Cr(VI) was prepared and was used to saturate the binding sites on the saltbush biomass. A 100-mg sample of the native saltbush biomass was washed twice with 0.01 M HCl to remove any debris and soluble materials; the biomass was then washed with DI water to remove any remaining acid. Part of the biomass was adjusted to pH 2.0, while the rest of the biomass was adjusted to pH 5.0. The biomass was reacted with 100 ml of the 1000 mg ml^{-1} of either Cr(III) or Cr(VI) solution at the same pH of the biomass and allowed to react for 1 h to saturate all the available binding sites. The pH of the 1000-mg ml^{-1} Cr(III) solution was adjusted to 5.0, while 500 ml of the Cr(VI) was adjusted to pH 5.0, and other 500 ml were adjusted at pH 2.0. After reaction, the samples were centrifuged at 3000 rpm for 5 min. Then the samples were washed with DI water to remove any unbound Cr from the samples and centrifuged again to pellet the biomass. The supernatants were decanted and discarded after the final washing. The samples were then frozen in liquid nitrogen for 60 min and lyophilized (LABCONCO Freeze Dry System/Freezone 4.5, Kansas City, MO, USA). The powdered samples were then packed into 1.0-mm aluminum sample plates with Kapton® tape windows for analysis at Stanford Synchrotron Radiation Laboratories (SSRL).

Table 1
ICP–OES operational parameters for the determination of Cr binding to saltbush biomass (*A. canescens*)

Wavelength	357.9 nm
Plasma flow	15 L min^{-1}
Auxiliary flow	0.2 L min^{-1}
Nebulizer flow	0.8 L min^{-1}
Pump rate	1.5 ml min^{-1}
RF power	1300 W

2.7.2. XAS data collection

All samples were run at SSRL on beam-line 7-3 using a liquid helium cryostat and the sample spectra were collected on the Cr K edge 5.989 keV. Sample spectra were collected using a 13-element germanium fluorescence detector. The operating conditions of the beam-line were as follows: a current ranging between 60 and 100 mA, energy of 3.0 GeV, and a Si double crystal monochromator (the Si 220 φ 90 monochromator was used). In addition, a 1.0-mm slit was used to reduce signal to noise ratios. The model compounds $K_2Cr_2O_7$, $Cr(NO_3)_3$, $Cr(PO_4)$ and $Cr(CH_3CH_2COO)_3$ were diluted using boron nitride to give a one absorption unit change across the absorption edge and transmission spectra were collected for all model compounds. The samples were diluted by grinding the model compounds and the boron nitride together using mortar and pestle until a homogenous mixture was obtained. The diluted model compounds were then packed into 1.0-mm aluminum sample plates with Kapton® tape windows.

2.7.3. XAS data analysis

The XAS data analysis was performed using the WinXAS software and standard methods [22]. The raw XAS spectra were first calibrated using the internal Cr metal standard, E_0 5.989 keV. Taking a second derivative of the Cr metal foil and correcting the energy of the spectra according to the inflection point of Cr metal from the literature, value performed to calibrate the samples and model compounds. After calibration, the samples were then background corrected using a two-polynomial fitting a one-degree polynomial to the pre-edge region and a fifth-degree polynomial to the post-edge region and the samples were normalized. The XANES region was then extracted from the sample and model compounds spectra by taking a section from 5.96 keV to 6.11 keV and the LC-XANES analysis was performed.

The EXAFS were extracted after background correction; the samples were converted into k space (wave vector space $Å^{-1}$). The conversion to k space was based on the energy of the photoelectrons ejected from the samples. The samples were then converted into k space based on this energy, using a spline of seven knots taken between 2.0 $Å^{-1}$ and 12.2 $Å^{-1}$, and the subsequent EXAFS curve was k weighted to three. The samples were then Fourier transformed and then back transformed and fitted using FEFF V8.00 and the appropriate model compounds [23]. The input files for the FEFF fitting were created using the Atoms software and crystallographic data in the literature [24]. The interatomic distances (R), coordination numbers (CN), and Debye–Waller factors (σ^2), were calculated using FEFF V8.00.

2.8. Statistical analyses

Each experiment was performed in triplicate for statistical purposes. 95% confidence intervals were calculated for the binding values in the pH profile experiments. The

binding data were analyzed using a one-way ANOVA followed by Tukey–HSD (honestly significant difference) test performed with the statistical package SPSS Version 11.0 (SPSS, 233 S. Wacker Drive, Chicago, IL).

3. Results and discussion

3.1. Effect of pH on Cr(III) and Cr(VI) binding by saltbush biomass

The percentages of Cr(III) and Cr(VI) bound by the native stems (NS), leaves (NL) and flowers (NF) of saltbush biomass are shown in Fig. 1A and B, respectively. As one can see in these figures, the binding for both chromium species was affected by the solution pH. For Cr(III), the percentages bound at pH values of 4.0 and 5.0 (greater than 90%) were statistically higher ($P<0.05$) than the percentages bound at pH 2.0 by the three tissues (35.7%, 49.6%, and 27.3% for the NS, NL, and NF, respectively). However, at pH 6.0 the percentage of Cr(III) bound by NL (79%) was statistically lower ($P<0.05$) than the percentages bound by this tissue at pH values of 3.0, 4.0, and 5.0 (89%, 97%, and 94%, respectively). On the other hand, differences were observed in the percentage of Cr(III) bound by the three tissues within each pH value. At pH values of 2.0 and 3.0, NL bound significantly more than NS and NF. However, at pH values of 5.0 and 6.0, NS bound more Cr(III) that NL and NF. These results might be explained by the number of binding sites available in the native biomass as a function of pH. On the other hand, the binding of Cr(VI) by NS, NL, and NF of saltbush plant decreased as pH increased. The percentages bound by each tissue at the pH values of 2.0 and 3.0 were statistically higher compared to the amounts

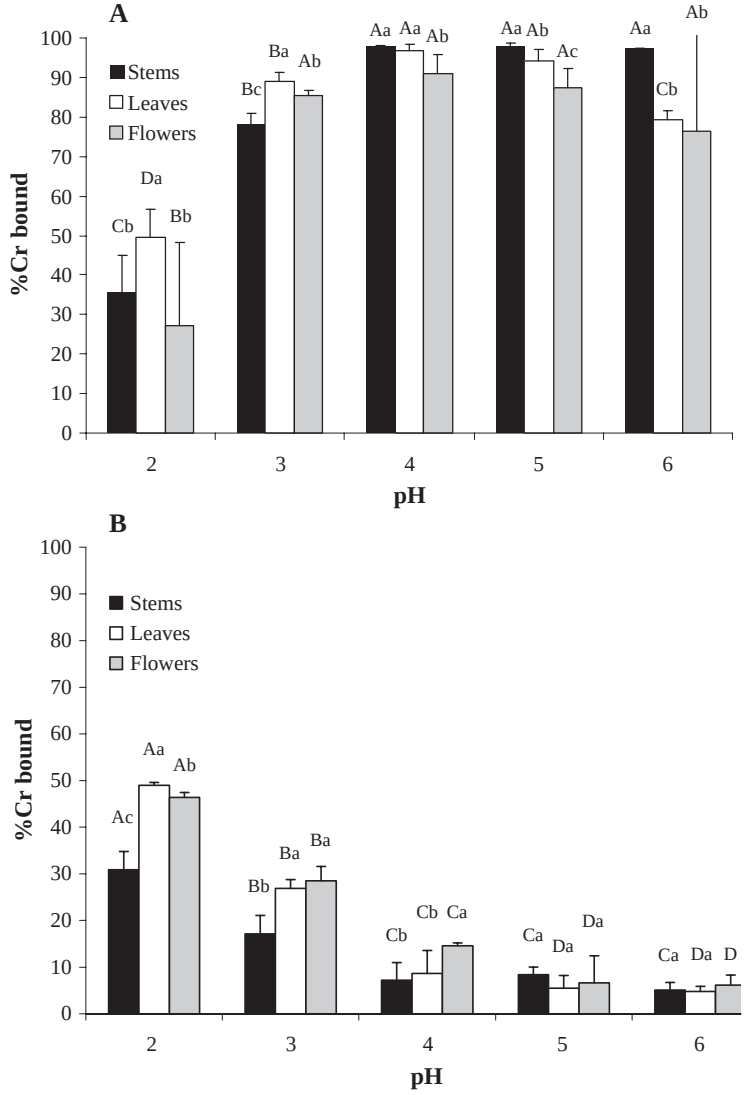

Fig. 1. pH profile for Cr(III) (A) and Cr(VI) (B) binding to native saltbush biomass (*A. canescens*). 5 mg ml^{-1} of biomass was reacted with 5.2 mg L^{-1} of Cr(III) and Cr(VI) separately. Lowercase letters indicate significant differences ($P<0.05$) in Cr content between tissues at the same pH. Uppercase letters indicate significant differences ($P<0.05$) in Cr content between tissues at different pH values. Error bars represent 95% confidence interval.

bound at the other pH values. As in the case of Cr(III), NS, NL, and NF behaved different within each pH value. At pH 2.0, NL bound statistically more Cr(VI) compared to NS and NF. However, at pH 4.0, NF bound significantly more Cr(VI) ($P<0.05$) than NS. No significant differences among the three tissues were observed at pH 5.0 and 6.0. Previous studies have shown that alfalfa [25] had the optimum Cr(III) binding at pH 5.0, and oat [16] had the highest binding of this metal at pH 6.0; however, the optimum pH for Cr(VI) binding by oat biomass [16] was 2.0.

The percentages of Cr(III) and Cr(VI) bound by esterified stems (ES), leaves (EL), and flowers (EF) of the saltbush plant are shown in Fig. 2A and B, respectively. As one can see in Fig. 2A, the Cr(III) binding by the three tissues increased as pH increased. The maximum percentage bound by ES biomass (95%) was reached at pH 6.0 and the minimum at pH 2.0 (13%). However, the maximum Cr(III) binding presented by EL biomass was reached at pH 6.0 (61%) and the lower at pH 2.0 (18%). While for EF biomass, the maximum binding (56%) was reached at pH 6.0 and the minimum at pH 2.0 (21%). On the other hand, the binding of Cr(VI) by esterified saltbush biomass was not affected by the pH. In all the cases, the percentage bound by ES biomass was statistically lower, compared to percentages bound by EL and EF biomasses (see Fig. 2B). As in the case of native biomass, the esterified tissues had different Cr(VI) adsorption ability within pH values. The percentage bound by ES at pH 2.0 (40%) was statistically higher ($P<0.05$) than the percentage bound at other pH values. On the other hand, at pH 2.0 and 3.0, EL bound statistically more Cr(VI) than ES and EF biomass ($P<0.05$). As mentioned before, it is hypothesized that these results could be explained

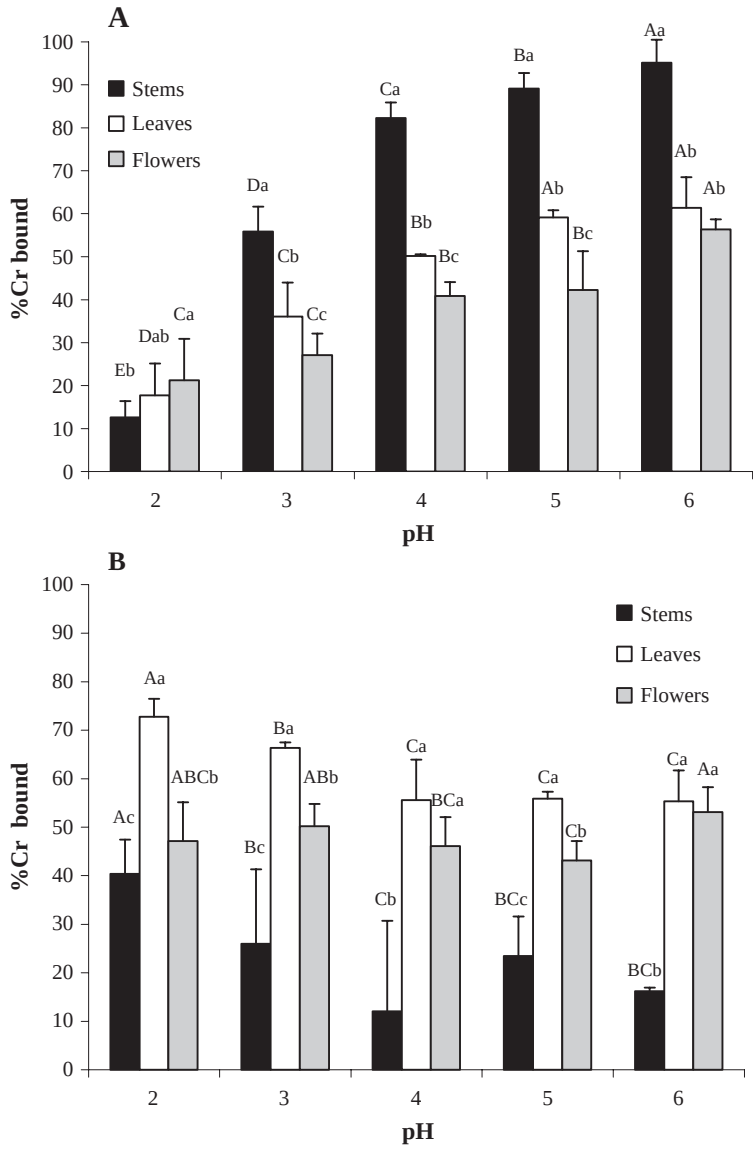

Fig. 2. pH profile for Cr(III) (A) and Cr(VI) (B) binding by esterified saltbush biomass (*A. canescens*). 5 mg ml^{-1} of biomass was reacted with 5.2 mg L^{-1} of Cr(III) and Cr(VI) separately. Lowercase letters indicate significant differences ($P<0.05$) in Cr content between tissues at the same pH. Uppercase letters indicate significant differences ($P<0.05$) in Cr content between tissues at different pH values. Error bars represent 95% confidence interval.

because each tissue has different number of binding sites or different functional groups that behave different at each pH values.

The percentages of Cr(III) and Cr(VI) bound by hydrolyzed stems (HS), leaves (HL), and flowers (HF) of the saltbush biomass are shown in Fig. 3A and B, respectively. Fig. 3A shows that each tissue bound almost the same amount of Cr(III) for pH values from 4.0 to 6.0. The percentages of Cr(III) bound at each pH value did not present statistical differences ($P<0.05$). At pH 2.0 the average of Cr(III) bound was about 68% and at pH 6.0 was about 96%. However, in general terms, the binding of Cr(VI) by hydrolyzed saltbush biomass decreased as pH increased. In the case of HS, the maximum percentage bound was found at pH 2.0 (28%) and the minimum at pH 4.0 (0.00). For the HL and HF biomass, the maximum percentage of Cr(VI) bound (about 47%) was reached at pH 2.0 and the minimum at pH 6.0 (about 7%). These percentages were statistically different ($P<0.05$). The results of these studies may indicate that the Cr binding to saltbush biomass could be via carboxyl groups present in the cell walls of the biomass (the pK_a for most of carboxyl groups range from 3.0 to 5.0) [26,27]. The differences among Cr(VI) and Cr(III) binding to the biomass might be due to the fact that Cr(VI) exists as an oxo-anion (CrO_4^{-2}, $Cr_2O_7^{-2}$), thus, if the carboxyl group is the main group involved in binding, a negatively charged ion will have less chance to be bound to a negatively charged ligand [16,25]. Therefore, the higher binding of Cr(VI) at low pH values could be explained through binding with a positively charged ligand like the amino groups, or by simultaneous anion exchange and reduction of Cr(VI) to Cr(III) [4]. Previous studies have shown that some types of biosorbents like seaweed, humic substances, oat, hops, and alfalfa have the ability to reduce Cr(VI) to Cr(III) [4,15,16,25,28]. The increase in the Cr(VI) binding by the esterified biomass could be due to a reduction in negative charges on the biomass after blocking the negatively charged carboxyl groups in the esterification process. The small increase in the Cr(VI) binding to the esterified stems suggests that the stems have less carboxyl groups than leaves and flowers. From Fig. 3B, nothing can be concluded about the ligand(s) responsible of the Cr(VI) binding by the esterified leaves and flowers, since there is no specific pH dependence trend. While for the stems, the functional group responsible for the binding could be a compound of low pK_a such as succinic

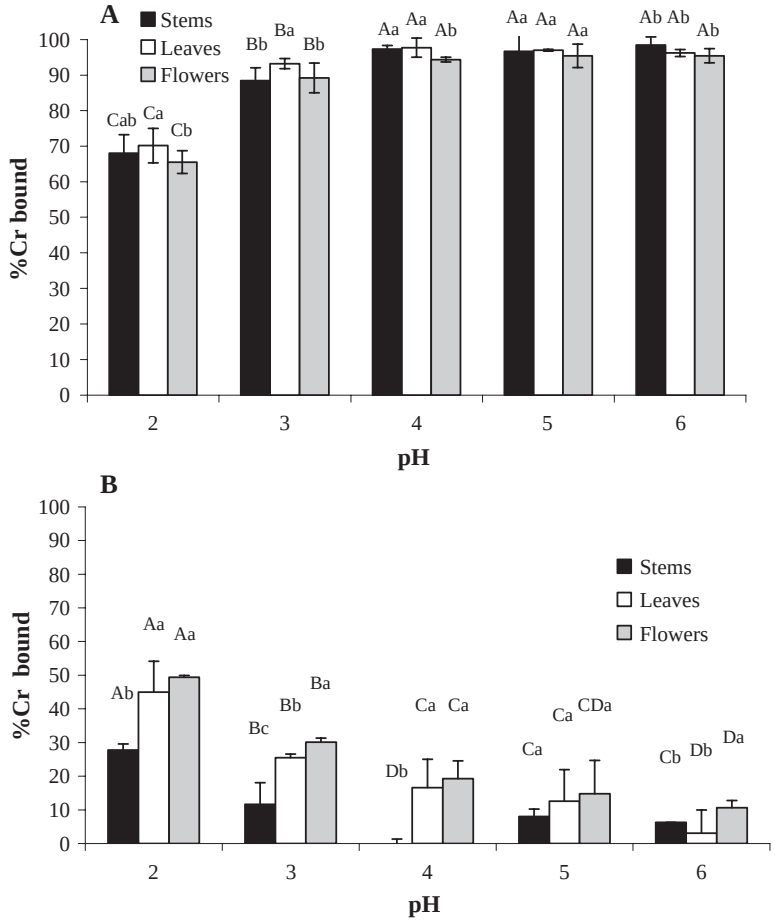

Fig. 3. pH profile for Cr(III) (A) and Cr(VI) (B) binding by hydrolyzed saltbush biomass (*A. canescens*). 5 mg ml^{-1} of biomass was reacted with 5.2 mg L^{-1} of Cr(III) and Cr(VI) separately. Lowercase letters indicate significant differences ($P<0.05$) in Cr content between tissues at the same pH. Uppercase letters indicate significant differences ($P<0.05$) in Cr content between tissues at different pH values. Error bars represent 95% confidence interval.

acid, arginine, or aspartic acid, which have pK_a's at or below 2.0, and contain the carboxyl functional groups that would not be greatly affected by the esterification process used in this study [29].

Comparing the hydrolyzed and native saltbush biomasses, it is possible to observe that at pH 2.0, there was an increase in Cr(III) binding of about 30%. This increase can be related to the conversion of the available ester groups into carboxyl groups by the hydrolysis process. For the pH range from 3.0 to 6.0, there was a small increase in the binding for the hydrolyzed biomass (about 6%) compared to the native biomass, this may be a function of the number of binding sites at these pH values and the relative concentration of metal ions. The results of the pH profile for the Cr(VI) binding with the hydrolyzed biomass show no significant difference from the native biomass, which can be due to the number of the carboxyl groups added after the hydrolyzation process and the repulsion between negative sites and the oxo-anion.

3.2. Saltbush biomass binding capacity for Cr(III) and Cr(VI)

The results of the Cr(III) and Cr(VI) binding capacity studies are shown in Table 2. This table shows that the NL biomass had an average binding capacity for Cr(III) of about 22.0 mg g^{-1}; the average of the hydrolyzed biomass was 25.0 mg g^{-1}, and the esterified 6 mg g^{-1}. These differences in binding capacity might be related to the relative number of carboxyl functional groups on the biomass. The esterification reduces the number of available carboxyl functional groups. It is clear that some of the oxygen-containing functional groups on the biomass seem to be affected by this treatment. Studies have shown that sorghum [30] had a Cr(III) adsorption capacity of 10 mg g^{-1}, alfalfa had an adsorption capacity of 7.7 mg g^{-1} [21,25], and 43.1 mg g^{-1} for *Solanum eleagnifolium* [31]. These data show that the saltbush plant could represent a better option compared to alfalfa and sorghum for the removal of Cr(III).

An inverse trend was observed for the Cr(VI) binding capacity of saltbush biomass. The esterified biomass had a higher Cr(VI) binding capacity compared to the native and hydrolyzed biomass. The Cr(VI) binding capacity of the native biomass had an average of about 0.1 mg g^{-1}, while the average of the hydrolyzed biomass was 0.2 mg g^{-1}, and the one of esterified was 3.6 mg g^{-1}. As explained before, the higher Cr(VI) binding capacity shown by the esterified biomass could be due to an overall smaller negative charges, compared to the native and hydrolyzed biomass. Saltbush showed to have a higher Cr(VI) adsorption capacity compared to nut shell (1.47 mg g^{-1}) [33], but lower than Irish peat moss (119 mg g^{-1}) [32]. Desorption studies are currently being performed to determine the best stripping agent for the bound chromium.

Table 2
Cr(III) and Cr(VI) binding capacity of saltbush biomass (*A. canescens*)

Biomass	Plant Part	Capacity (mg g^{-1})	
		Cr(III)	Cr(VI)
Native	Stems	16.3±0.06	0.0±0.06
	Leaves	22.7±0.12	0.1±0.04
	Flowers	27.0±0.12	0.1±0.04
Esterified	Stems	5.5±0.06	3.4±0.26
	Leaves	6.1±0.06	4.1±0.08
	Flowers	7.1±0.07	3.1±0.06
Hydrolyzed	Stems	20.8±0.15	0.0±0.05
	Leaves	25.1±0.13	0.4±0.06
	Flowers	26.2±0.20	0.3±0.06

Data are averages of 10 saturation cycles±95% confidence intervals. Reactions were performed at pH 5.

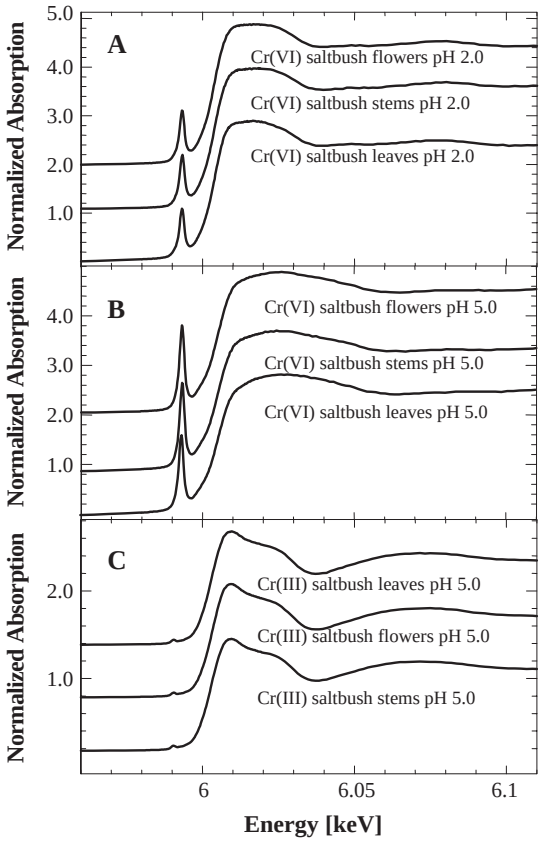

Fig. 4. XANES region of Cr(VI) reacted with native saltbush plant (*A. canescens*) parts flowers, stems, and leaves: (A) at pH 2.0 and (B) at pH 5.0. (C) XANES region of Cr(III) reacted with native saltbush plant parts flowers, stems, and leaves at pH 5.0.

Fig. 4A–C show the XANES of the Cr(VI) reacted with saltbush biomass at pH 2.0 and pH 5.0, and Cr(III) at pH 5.0, respectively. As can be seen in Fig. 4A and B, at pH 2.0 the amount of Cr present on the biomass in the VI oxidation state is lower compared to the amount of this oxidation state on the biomass at pH 5.0. The reduction in the oxidation state of Cr(VI) reacted with biomass has been observed in the Cr K-edge XANES for a number of different biomaterials [4,16,34,35]. In Fig. 4C, the XANES results of the reaction of Cr(III) with the different parts of the saltbush biomass, show a small pre-edge feature. The pre-edge

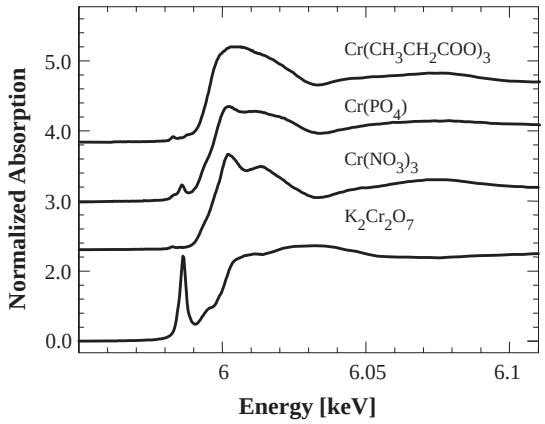

Fig. 5. XANES of Cr(III) and Cr(VI) model compounds; $K_2Cr_2O_7$, $Cr(NO_3)_3$, $Cr(PO_4)$, and $Cr(CH_3CH_2COO)_3$.

feature is indicative of Cr(III) bound to oxygen ligands in an octahedral arrangement of atoms [36]. Thus the results presented in Fig. 4 are indicating that chromium bound to the biomass is present in a octahedral arrangement of oxygen atoms. Fig. 5 shows the XANES of the model compounds potassium dichromate, Cr(III) phosphate, Cr(III) acetate, and Cr(III) nitrate. Similar pre-edge features are observed in the Cr(III) model compounds and the chromium samples (Fig. 4). An enlargement of the

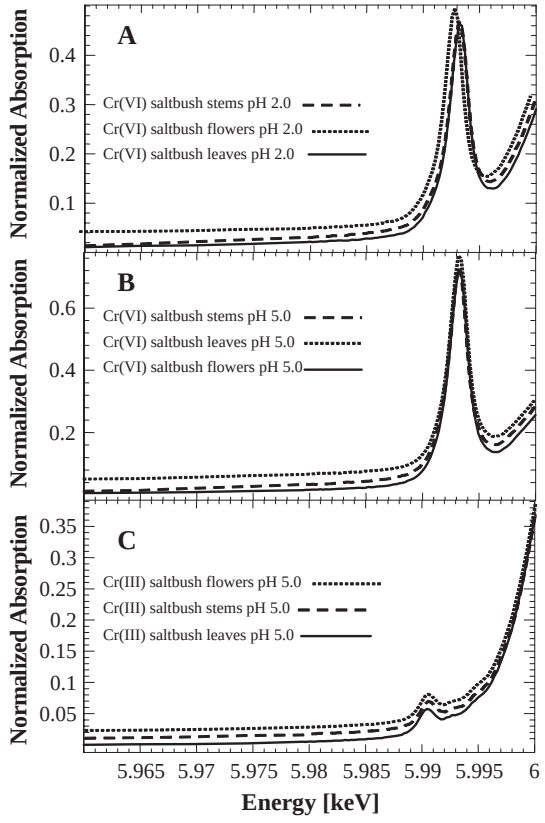

Fig. 6. Pre-edge region of Cr(VI) reacted with native saltbush plant (*A. canescens*) parts flowers, stems, and leaves: (A) at pH 2.0 and (B) at pH 5.0. (C) Pre-edge region of Cr(III) reacted with ground saltbush plant parts flowers, stems, and leaves at pH 5.0.

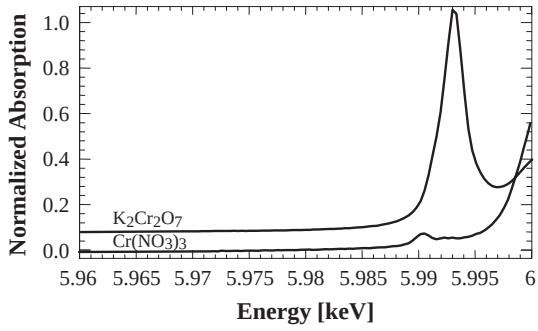

Fig. 7. Representative pre-edge features observed in the XANES spectra of the Cr(VI) and Cr(III) samples, Cr(III) nitrate, and potassium dichromate.

chromium pre-edge features is shown in Fig. 6A–C with the representative pre-edge features and the model compounds potassium dichromate and Cr(III) nitrate are shown in Fig. 7. As can be seen in Fig. 7, the Cr(VI) pre-edge feature is approximately 1 absorption unit in height, which corresponds to a sample that is 100 percent Cr(VI) [16,37]. The samples that were reacted with Cr(VI) at pH 2.0 and at pH 5.0 show varying amounts of Cr(VI) present in the sample. At pH 5.0, the average Cr(VI) observed in the samples varied from 80% to 60%, meaning that the other 20% to 40% was Cr(III), as was shown by the LC-XANES fittings (Table 3). However, the Cr(VI) samples that were reacted at pH 2.0 with the saltbush plant tissues show a greater reduction in the percentage of Cr(VI) present on the plant, compared to the samples reacted at pH 5.0. The reduction of the Cr(VI) is shown in Fig. 6A, from the reduction in height of the Cr(VI) pre-edge feature, which was confirmed by the LC-XANES fittings shown in Table 3. As can be seen in Fig. 6A, at pH 2.0, approximately 40% of the chromium remains as Cr(VI) on the plant tissues. The increase in the reduction of the Cr(VI) on the plant at pH 2.0 is to be expected as Cr(VI) has a much higher oxidative power at lower pH. The pre-edge feature of the Cr(III) reacted with the saltbush biomass tissues shown in Fig. 6C is almost identical to the Cr(III) nitrate model compound pre-edge feature shown in Fig. 7. As mentioned earlier, the Cr(III) pre-edge feature is indicative of Cr(III) bound to oxygen ligands in an octahedral arrangement [35]. However, the XANES continuum of the samples and the Cr(III) nitrate (an octahedral arrangement of oxygen atoms around the

Table 3
LC-XANES fittings of the pre-edge features observed in the chromium–saltbush biomass (*A. canescens*) samples

Sample	%Cr(III)±SE%	%Cr(VI)±SE%
Cr(VI) saltbush flowers pH 2	59.8±5.6	40.2±0.8
Cr(VI) saltbush leaves pH 2	55.9±5.6	44.1±1.0
Cr(VI) saltbush stems pH 2	61.2±6.0	38.8±0.9
Cr(VI) saltbush flowers pH 5	20.5±2.09	79.5±1.94
Cr(VI) saltbush leaves pH 5	37.4±3.5	62.5±1.2
Cr(VI) saltbush stems pH 5	38.4±5.4	61.6±1.3
Cr(III) saltbush flowers pH 5	96.9±9.8	3.1±0.05
Cr(III) saltbush leaves pH 5	97.4±8.7	2.6±0.03
Cr(III) saltbush stems pH 5	97.4±10.0	2.6 ±0.04

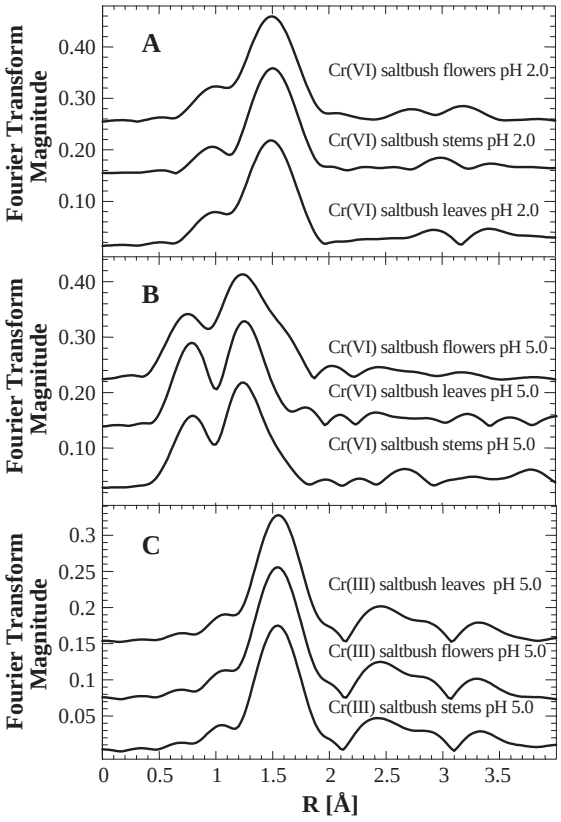

Fig. 8. EXAFS region of Cr(VI) reacted with ground saltbush plant (*A. canescens*) parts flowers, stems, and leaves: (A) at pH 2.0 and (B) at pH 5.0. (C) EXAFS region of Cr(III) reacted with ground saltbush plant parts flowers, stems, and leaves at pH 5.0.

Cr(III) center) are not identical, indicating that the coordination is somewhat different. The amplitude of the features in the Cr(III) samples are dampened, indicating that the assembly of oxygen atoms around the central Cr(III) atom is in a distorted octahedral arrangement [38].

The results of the EXAFS studies for Cr(VI) and Cr(III) reacted with the saltbush plant sections are shown in Fig. 8A–C. The EXAFS of the model compounds are shown in Fig. 9. Tables 4 and 5 show the FEFF fittings of the

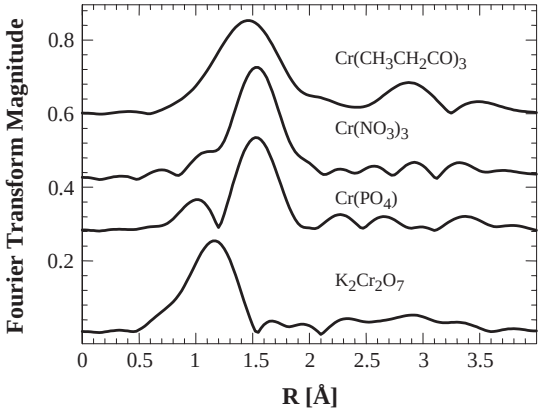

Fig. 9. Fourier transformed EXAFS of Cr(III) and Cr(VI) model compounds: $K_2Cr_2O_7$, $Cr(NO_3)_3$, $Cr(PO_4)$, and $Cr(CH_3CH_2COO)_3$.

Table 4
FEFF fittings of chromium(III) and chromium(VI) binding to the saltbush biomass (*A. canescens*) in individual and in mixed solution of the chromium(III) and chromium(VI)

Sample	Bond	CN[a]	R (Å)	σ^2 (Å^2)
Cr(VI) saltbush flowers pH 2	Cr–O	1.8	1.74	0.0090
	Cr–O	3.2	1.95	0.0087
Cr(VI) saltbush leaves pH 2	Cr–O	1.8	1.84	0.0067
	Cr–O	3.4	2.07	0.0067
Cr(VI) saltbush stems pH 2	Cr–O	1.2	1.80	0.0040
	Cr–O	3.0	2.00	0.0043
Cr(VI) saltbush flowers pH 5	Cr–O	3.1	1.80	0.0074
	Cr–O	2.1	2.05	0.0012
Cr(VI) saltbush leaves pH 5	Cr–O	3.4	1.83	0.014
	Cr–O	2.1	2.06	0.0030
Cr(VI) saltbush stems pH 5	Cr–O	3.0	1.77	0.020
	Cr–O	1.9	2.13	0.0037
Cr(III) saltbush leaves pH 5	Cr–O	5.7	2.01	0.0070
Cr(III) saltbush stems pH 5	Cr–O	5.6	2.02	0.0071
Cr(III) saltbush flowers pH 5	Cr–O	6.0	2.01	0.0065

[a] CN represents the coordination number, R is the interatomic distances given in angstroms, and σ^2 is the Debye–Waller factor given in angstroms squared.

backtransformed EXAFS of the chromium–saltbush samples and the chromium model compounds, respectively. The EXAFS of the Cr(VI) reacted with saltbush biomass at pH 2.0 and pH 5.0 shows that both Cr(VI) and Cr(III) are coordinated to oxygen ligands (Fig. 8A and B). The main oscillation in the FT-EXAFS for the Cr(VI) reacted with the saltbush plants at pH 5.0 is shifted to an interatomic distance between that of Cr(VI)–oxygen bond length (1.65 Å) and Cr(III)–oxygen bond length (1.95 Å). In addition, the Cr(VI) reacted with the saltbush biomass tissues are distorted in their appearance showing the mixture of both Cr(III) and Cr(VI). However, the higher percentage of Cr(VI) in these samples is apparent compared to the samples reacted at pH 2.0. The Cr(VI) samples reacted at pH 2.0 with the saltbush biomass parts show interatomic distances close to that of Cr(III), indicating a higher concentration of Cr(III), as seen in the XANES analysis. However, the EXAFS oscillations of the Cr(VI) reacted at pH 2.0 with the

Table 5
FEFF fittings of Cr(III) and Cr(VI) model compounds: $K_2Cr_2O_7$, $Cr(NO_3)_3$, $Cr(PO_4)$, and $Cr(CH_3CH_2COO)_3$

Sample	Bond	CN[a]	R (Å)	σ^2 (Å^2)
$K_2Cr_2O_7$	Cr–O	2.01	1.65	0.0038
	Cr–O	1.2	1.67	0.0036
	Cr–O	0.9	1.83	0.0075
$Cr(NO_3)_3$	Cr–O	6.0	1.97	0.0017
$Cr(PO_4)$	Cr–O	2.5	1.93	0.0011
	Cr–O	3.1	2.01	0.0029
	Cr–P	3.2	3.22	0.0070
	Cr–P	2.9	3.50	0.0061
$Cr(CH_3CH_2COO)_3$	Cr–O	5.9	1.96	0.00081
	Cr–C	7.1	3.44	0.0011

[a] CN represents the coordination number, R is the interatomic distances given in angstroms, and σ^2 is the Debye–Waller factor given in angstroms squared.

saltbush are somewhat distorted compared to the Cr(III) samples reacted with this biomass. The fittings of the EXAFS are shown in Table 4, which indicate the presence of both Cr(VI) and Cr(III) in the Cr(VI) samples as indicated by the two variable chromium–oxygen bond lengths at approximately 1.8 Å and 1.95–2.0 Å. The variable bond length is confirming the results of the XANES analysis that both oxidation states are present in the samples. In addition, the results of the EXAFS fittings for the Cr(III) reacted with the saltbush biomass tissues also confirm the results of the XANES analysis for these samples. The fitting results show only the presence of Cr(III) bound to oxygen ligands in an octahedral arrangement of atoms as did the results of the EXAFS fittings of Cr(III) nitrate, Cr(III) phosphate and Cr(III) acetate shown in Fig. 5 and Table 5.

4. Conclusions

The results of these studies demonstrated that native saltbush biomass can remove more than 90% of the Cr(III) from an aqueous solution at pH values of 4.0 and 5.0. The results also demonstrated that hydrolyzed saltbush biomass adsorbed more than 90% of the Cr(III) ions in a pH range from 3.0 to 6.0. In addition, the esterified biomass of leaves was able to adsorb more than 50% of the Cr(VI) present in the aqueous solution. The capacity experiments support the idea that the carboxyl groups present on the cell wall of the saltbush biomass are not the groups that play the major role in Cr binding by the stems, but by the leaves and the flowers. The results of the XAS experiments showed that the Cr(VI) reacted with the saltbush plant sections at both pH 2.0 and pH 5.0 was reduced to some extent to Cr(III). The EXAFS results for these samples also show a reduction in the oxidation state, from the mixed bond lengths in the FEFF fitting results. The results of the XANES analysis of the Cr(III) reacted with the saltbush plant tissues showed that the samples are in an octahedral arrangement of oxygen atoms around the central Cr(III) atom. This was further shown in the results of the EXAFS studies of these samples.

Acknowledgments

The authors would like to acknowledge the National Institutes of Health (grant S06 GM8012-33) and the University of Texas at El Paso's Center for Environmental Resource Management (CERM) through funding from the Office of Exploratory Research of the U.S. Environmental Protection Agency (cooperative agreement CR-819849-01). We also thank the financial support from the Southwest Center for Environmental Research and Policy (SCERP) program, and the HBCU/MI, Environmental Technology Consortium that is funded by the Department of Energy. Dr. Gardea-Torresdey acknowledges the funding from the National Institute of Environmental Health Sciences (Grant R01ES11367-01) and the Dudley family for the Endowed Research Professorship in Chemistry. Portion of this research was carried out at the Stanford Synchrotron Radiation Laboratory (SSRL), a national user facility operated by Stanford University on behalf of the US Department of Energy (DOE), Office of Basic Energy Sciences. The Authors also thank Mr. J.H. Gonzalez for his help in metal quantification using the ICP. Maather Sawalha also acknowledges the financial support of the Fulbright Foreign Student Program through the administration of AMIDEAST.

References

[1] S.E. Bailey, T.J. Olin, R.M. Bricka, D.D. Adrian, Water Res. 33 (1999) 2469.
[2] R.S. Bai, T.E. Abraham, Water Res. 36 (2002) 1224.
[3] A.R. Sardashti, Water Wastewater 45 (2003) 18.
[4] D. Kratochvil, P. Pimentel, B. Volesky, Environ. Sci. Technol. 32 (1998) 2693.
[5] E.T. Snow, Environ. Health Perspect. 92 (1991) 75.
[6] F. Forster, J. Wase (Eds.), Biosorbents for Metal Ions, Taylor & Francis Ltd, UK, 1997.
[7] R. Machado, J.R. Carvalho, M.J. Correia, J. Chem. Technol. Biotechnol. 77 (2002) 1340.
[8] J.L. Nyman, F. Caccavo Jr., Biorem. J. 6 (2002) 39.
[9] R.S. Bai, T.E. Abraham, Bioresour. Technol. 87 (2003) 17.
[10] W.P. Anderson, Ion Transport in Plant, Academic Press, London, 1973, p. 340.
[11] B. Volesky, Hydrometallurgy 59 (2001) 203.
[12] M. Tsezos, A.A. Deutschmann, J. Chem. Technol. Biotechnol. 48 (1990) 29.
[13] M. Fomina, G.M. Gadd, J. Chem. Technol. Biotechnol. 78 (2003) 23.
[14] J. Gardea-Torresdey, M. Hejazi, J.G. Parsons, K. Tiemann, J. Henning, Preprints of Extended Abstracts Presented at the ACS National Meeting, vol. 41, 2001, p. 441.
[15] J.G. Parsons, M. Hejazi, K.J. Tiemann, J. Henning, J.L. Gardea-Torresdey, Microchem. J. 71 (2002) 211.
[16] J.L. Gardea-Torresdey, K.J. Tiemann, V. Armendariz, L. Bess-Oberto, R.R. Chianelli, J. Rios, J.G. Parsons, G. Gamez, J. Hazard. Mater. 80 (2000) 175.
[17] S. Schiewer, B. Volesky, Environ. Microbe-Metal Interact. (2000) 329.
[18] U. Luettge, in: A. Laeuchi, U. Luettge (Eds.), Salinity, Kluwer Academic Publishers, Dordrecht, Neth, 2002, p. 341.
[19] J.L. Gardea-Torresdey, M.K. Becker-Hapak, M.J. Hosea, D.W. Darnall, Environ. Sci. Technol. 24 (1990) 1372.
[20] J.L. Gardea-Torresdey, L. Tang, J.M. Salvador, J. Hazard. Mater. 48 (1996) 191.
[21] J.L. Gardea-Torresdey, K.J. Tiemann, J.H. Gonzales, I. Cano-Aquilera, J.A. Henning, M.S. Townsend, J. Hazard. Mater. 49 (1996) 205.
[22] T. Ressler, J. Synchrotron Radiat. 5 (1998) 118.
[23] A.L. Ankudinov, B. Ravel, J.J. Rehr, S.D. Conradson, Phys. Rev., B, Condens. Matter Mater. Phys. 58 (1998) 7565.
[24] B. Ravel, J. Synchrotron Radiat. 8 (2001) 314.
[25] J.L. Gardea-Torresdey, J.H. Gonzalez, K.J. Tiemann, O. Rodriguez, G. Gamez, J. Hazard. Mater. 57 (1998) 29.
[26] N. Kuyucak, B. Volesky, Water Pollut. Res. J. Can. 23 (1988) 424.
[27] Y.-S. Yun, D. Park, J.M. Park, B. Volesky, Environ. Sci. Technol. 35 (2001) 4353.
[28] P.R. Wittbrodt, C.D. Palmer, Environ. Sci. Technol. 30 (1996) 2470.
[29] G.D. Fasman, Handbook of biochemistry: section D physical chemical data, vol. I, 3rd ed., CRC Press, Cleveland, OH, 1976, p. 427.

[30] I. Cano-Rodriguez, J.A. Perez-Garcia, M. Gutierrez-Valtierra, J.L. Gardea-Torresdey, Rev. Mex. Ing. Quim. 1 (2002) 97.
[31] K.J. Tiemann, A.E. Rascon, G. Gamez, J.G. Parsons, T. Baig, I. Cano-Aguilera, J.L. Gardea-Torresdey, Microchem. J. 71 (2002) 133.
[32] Y.S. Ho, D.A. Wase, C.F. Forster, Water Res. 29 (1995) 1327.
[33] Y. Orhan, H. Buyukgungor, Water Sci. Technol. 28 (1993) 247.
[34] Z.-Y. Lin, J.-K. Fu, J.-M. Wu, Y.-Y. Liu, H. Cheng, Wuli Huaxue Xuebao 17 (2001) 477.
[35] K. Dokken, G. Gamez, I. Herrera, K.J. Tiemann, N.E. Pingitore, R.R. Chianelli, J.L. Gardea-Torresdey, in: L.E. Erickson, D.L. Tillison, S.C. Grant, J.P. McDonald (Eds.), Proc. Conf. Hazard. Waste Res., St. Louis, MO, 1999, p. 101.
[36] M.L. Peterson, G.E. Brown, G.A. Parks, C.L. Stein, Geochim. Cosmochim. Acta 61 (1997) 3399.
[37] C.M. Lytle, F.W. Lytle, N. Yang, J.-H. Qian, D. Hansen, A. Zayed, N. Terry, Environ. Sci. Technol. 32 (1998) 3087.
[38] D.C. Koningsberger, R. Prins (Eds.), Chemical Analysis, X-ray Absorption: Principles, Applications, Techniques of EXAFS SEXAFS, and XANES, vol. 91, John Wiley & Sons, New York, 1988.